Atmósfera 39, 143-167 (2025)
https://doi.org/10.20937/ATM.53396

Performance evaluation of random forest and boosted tree in rainfall-runoff process modeling for sub-basins of Lake Urmia

Zeinab BIGDELI, Abolfazl MAJNOONI-HERIS*, Reza DELIRHASANNIA and Sepideh KARIMI

Department of Water Engineering, University of Tabriz, East Azerbaijan Province, Tabriz, 29 Bahman Boulevard, Irán.
*Corresponding author; email: majnooni@tabrizu.ac.ir

Received: April 28, 2024; Accepted: November 8, 2024

RESUMEN

Este estudio tuvo como objetivo desarrollar modelos de lluvia-escorrentía (P-Q) utilizando modelos de aprendizaje automático en las subcuencas del lago Urmia, Irán. En esta investigación se analizaron registros cronológicos de parámetros hidrológicos y datos meteorológicos a escala regional utilizando métodos heurísticos de bosque aleatorio (RF) y árbol potenciado (BT). Este estudio comparó el desempeño de estos dos modelos para la cuenca del Urmia durante el período 1976-2019. Los resultados mostraron que el modelo RF proporcionó mejores estimaciones en las estaciones de Akhula, Daryan y Ghermez Gol en la subcuenca oriental, y en las estaciones de Miandoab, Pole ozbak, Abajalu Sofla, Nezam Abad y Pole Bahramlu en la subcuenca occidental. En cambio, el modelo BT tuvo un mejor desempeño en las estaciones Pole Senikh, Shishvan, Gheshlagh Amir, Shirin Kandi y Khormazard en la subcuenca oriental y en las estaciones Babarud, Keshtiban y Yalghoz Aghaj en la subcuenca occidental. Además, el análisis de series temporales mostró cambios en la frecuencia anual de precipitaciones y una tendencia decreciente en el caudal en la mayoría de los años. Estos hallazgos destacan una reducción significativa en el caudal de entrada al lago Urmia en los últimos 43 años, con una disminución particularmente pronunciada en los últimos años.

ABSTRACT

This study aimed to develop rainfall-runoff (P-Q) modeling using machine learning models in the sub-basins of Lake Urmia, Iran. In this research, chronological records of hydrological parameters and meteorological inputs at a regional scale were analyzed using Random Forest (RF) and Boosted Tree (BT) heuristic methods. This study compared the performance of these two models for the Urmia Basin over the period from 1976 to 2019. The results showed that the RF model provided better estimates in Akhula, Daryan, and Ghermez Gol stations in the eastern sub-basin and Miandoab, Pole Ozbak, Abajalu Sofla, Nezam Abad, and Pole Bahramlu stations in the western sub-basin. In contrast, the BT model performed better at Pole Senikh, Shishvan, Gheshlagh Amir, Shirin Kandi, and Khormazard stations in the eastern sub-basin and Babarud, Keshtiban, and Yalghoz Aghaj stations in the western sub-basin. Additionally, the time series analysis showed changes in yearly rainfall frequency and a decreasing trend in flow discharge in most years. These findings highlight a significant reduction in inflow to Lake Urmia over the past 43 years, with a particularly sharp decline in recent years.

Keywords: rainfall-runoff, modeling, machine learning, Urmia lake, Boosted Tree, Random Forest.

1. Introduction

The need for meticulous planning in water resource conservation and utilization is underscored by rapid population growth and adverse environmental conditions (Aktürk and Yıldız , 2018; Tayyab et al., 2019; Ali and Shahbaz, 2020; Obasi et al., 2020). In hydrology, predictive modeling using flow data from water basins has demonstrated significant potential (Sun et al., 2019; Adnan et al., 2020). However, the nonlinear nature of hydrological data, including flow data, presents challenges in calculations and modeling (Kumar et al., 2019). Previous research commonly employs observed rainfall and runoff data to estimate output values using flow data (Singh et al., 2018; Turhan et al., 2019; Vidyarthi et al., 2020). Lake Urmia, situated in Iran's north-western region, has experienced a substantial decrease in water level, dropping by up to 5 m in the last 45 years, attributed to factors such as climate change, overexploitation of water resources, dam construction, and reduced rainfall in the lake basin (Hassanzadeh et al., 2012). The outflow of rivers into the lake is pivotal in disrupting the stability of inflow and outflow. Predicting river inflow necessitates extensive studies to forecast rainfall levels over the basin in the coming years. However, the hydrological complexity makes it challenging to understand the correlation between rainfall and runoff (Wang et al., 2013). The R-R model, pivotal in accurately modeling rain-runoff relationships, presents a significant challenge with wide-ranging applications in water resource management, hydropower generation, irrigation, urban planning, and agrohydrological/meteorological activity planning (Alizadeh et al., 2017). To address the limitations of traditional time series models, a new class of regression models based on machine learning techniques has emerged, including Support Vector Machine (SVM), Random Forest (RF), Boosted-Tree (BT), and Multivariate Adaptive Regression Splines (MARS) (Kisi and Parmar, 2016). Park and Markus (2014) and Meng et al. (2016) identified three common models for modeling the relationship between rainfall and runoff: conceptual models, physically grounded models, and black box models. As defined by Lee et al. (2005), a conceptual model represents a network of concepts used to estimate, recreate, or understand the subject being modeled. Physically based models, as described by Calver (1988), are physical replicas of objects used to study hydrological processes. According to Kan et al. (2016), black box models are systems that allow for interrogating their inputs and outputs without requiring knowledge of their internal workings. Conceptual and physically grounded models are widely regarded as the most suitable approaches for understanding the relationship between rainfall and runoff.

Machine learning and modern approaches have gained significant traction in water resources studies, with RF and BT algorithms emerging as crucial methods for making multiple predictions. RF, an ensemble model composed of numerous BTs, has found widespread application in various fields, including environmental and water resource management (Breiman, 2001; Norouzi et al., 2018). Additionally, the BT approach, particularly for the regression model, has demonstrated efficiency in ecological modeling within hydrological regions (Nylén et al., 2014). Lee et al. (2017) conducted a study on spatial flood vulnerability prediction in metropolitan Seoul, Korea, employing RF and BT models. The RF model achieved validation accuracies of 78.78% for the regression algorithm and 79.18% for the classification algorithm, while the BT model attained validation accuracies of 77.55 and 77.26%, respectively. In the literature, several studies have applied machine learning methods in rainfall-runoff modeling in the Urmia Lake basin. Farajzadeh et al. (2014) compared monthly rainfall and runoff modeling in the Lake Urmia basin using two approaches: the "feed-forward neural network" and the "time series analysis" model. They calculated the runoff coefficient regime based on parallel rainfall data over the basin for 39 years and predicted future runoff from the forecasted rainfall. Shiri (2019) studied prediction vs. estimation of dewpoint temperature (T_{dew}) by assessing the Gene Expression Programming (GEP), Multivariate Adaptive Regression Spline (MARS), and Random Forest (RF) models. This study develops T_{dew} models using GEP, MARS, and RF with data from six weather stations in East Azerbaijan, Iran, over 10 years. GEP models excelled in predicting T_{dew} at daily and weekly intervals, while MARS models, using air temperature, relative humidity, and sunshine hours, were most accurate for estimating T_{dew}. The study recommends MARS for estimation and highlights issues with using single data sets for analysis.

Asadi et al. (2019) utilized data-driven models based on artificial neural networks (ANNs) to estimate monthly runoff, achieving improved accuracy by incorporating hydrogeomorphic and biophysical time series inputs. Li et al. (2020) investigated the impact of forest change on annual runoff estimation using a statistical approach based on RF, revealing varied increases in the projected runoff across catchments. Karimi et al. (2020) surveyed supplanting missing climatic inputs in classical and RF models for estimating reference evapotranspiration in humid coastal areas of Iran. This study evaluates the impact of estimated meteorological variables on the accuracy of the Penman-FAO-Monteith (PFM) equation and empirical evapotranspiration (ETo) models. It uses 10 years of daily data from six humid coastal locations in Iran. The study finds that replacing missing inputs with estimated values improves accuracy, especially when estimated wind speed values are used. However, using estimated solar radiation values can reduce model accuracy.

Additionally, the study compares these results with machine learning models, specifically bootstrap aggregating-based RF under the same conditions. Tariq et al. (2021) explored the application of machine learning techniques for rainfall-runoff modeling in the Soan river basin in Pakistan, underscoring the importance of factors such as pool characteristics, geography, and composition in influencing the outcomes of the wavelet approach. Thus, careful selection of the wavelet family, type, and decomposition degree is crucial for optimal results. In another study, Turhan (2021) compared the effectiveness of ANNs in modeling the rainfall-runoff relationship for water resources management. Focusing on the Nergizlik dam in the Seyhan sub-basin in Turkey, the study found that ANN techniques produced statistically valid conclusions in rain-runoff modeling, with the developed models being successfully applied to evaluate medium monthly runoff. Bigdeli et al. (2023) studied the application of SVM and the BT algorithm for rainfall-runoff modeling at Tabriz Plain. The results showed that, during the study periods, the SVM model outperformed the BT model at Akhula station, while the BT model performed better than SVM model for Pole Senikh station. In the last study, Bigdeli et al. (2024) surveyed rain-runoff modeling of Khormazard and Bonab hydrometric stations using SVM and RF algorithms. In this research, rainfall-runoff simulation of Khormazard and Banab stations (on Sufichai and Mahperichai rivers) was carried out using data mining models of SVM and RF models. The results showed that in the Bonab station, the SVM model had higher efficiency than the RF model, and in the Khormazard station, the latter model provided better performance than SVM model during the study periods.

The literature lacks descriptions of rainfall-runoff modeling in the Lake Urmia basin using heuristic models. This study focuses on the application and validation of RF and BT heuristic methods in the all-sub-basins of Lake Urmia, utilizing chronological records of parameters and regional-scale meteorological inputs. The significance of each variable was computed, and RF and BT models were compared. The RF and BT models were chosen for rainfall-runoff modeling in the Urmia Lake basin because these models had not been previously applied in this region. The aim is to obtain more accurate predictions of monthly discharge, prioritizing the most practical and available model based on hydrological insights. Also, this study represents the first application of RF and BT models to predict/estimate the rainfall-runoff from 16 key Lake Urmia Basin stations.

2. Methodology

2.1 Study area and data description

Lake Urmia Basin, located at 44º 07'-47º 53' E longitude and 35º 40'-38º 30' N latitude, is one of the six main basins of Iran, with a total size of 52 679 km^2. The basin encompasses 34 000 km^2 of mountainous terrain and 13 000 km² of flat terrain, with 6000 km^2 dedicated to arable land and orchards. The remaining 5000 km^2 of the basin is occupied by Lake Urmia, which is considered a huge water body in Iran. Figure 1 shows the Lake Urmia basin along with its river network and hydrometric stations. Daily, monthly, and yearly rainfall and runoff data were provided by two Iranian institutions: the Iran Meteorological Organization and the Regional Water Company of East Azerbaijan. This data, spanning 43 years (1976-2019), was collected from 228 rain gauge stations within and around the lake and from 16 major runoff gauge stations leading into the Lake Urmia basin. The selected stations for our study were Akhula,

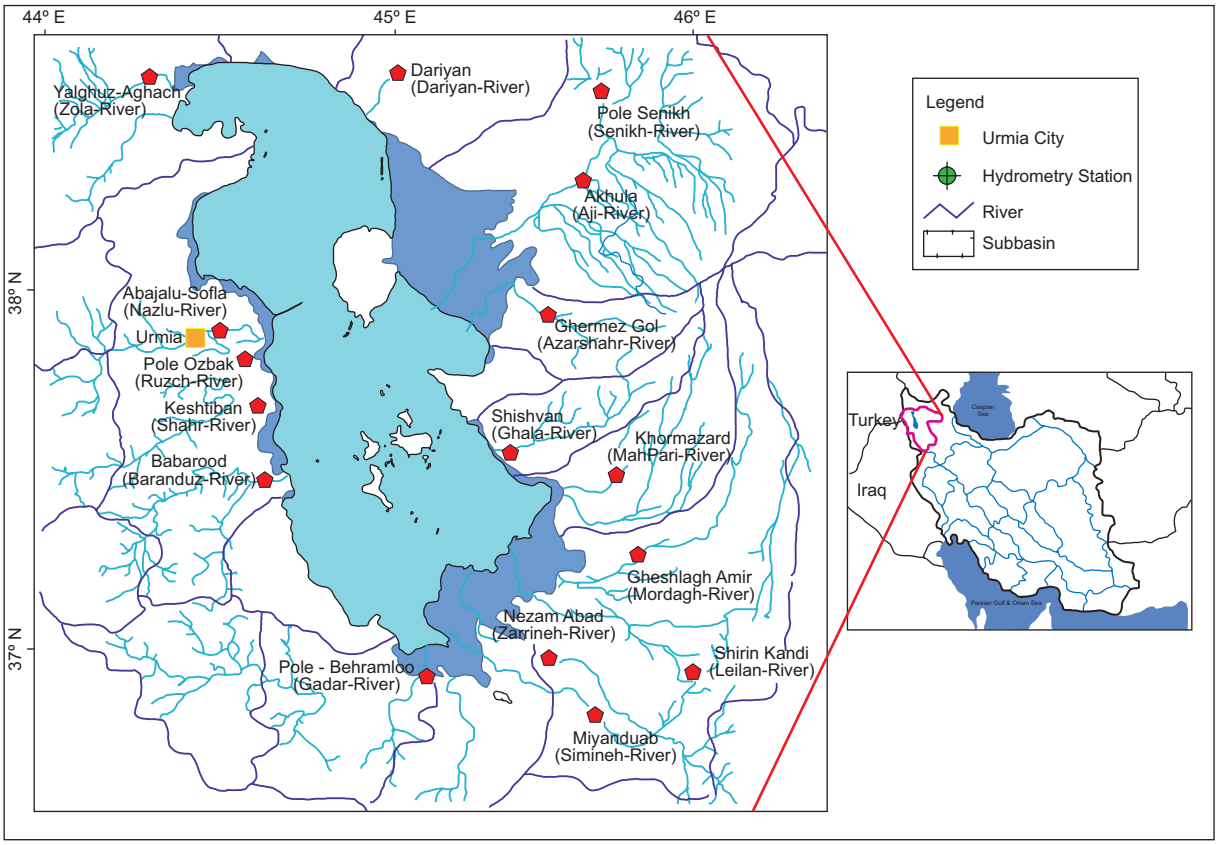

Fig. 1. Lake Urmia basin with river network and hydrometric stations.

Daryan, Pole Senikh, Shishvan, Gheshlagh Amir, Ghermez Gol, Shirin Kandi, Khormazard, Miandoab, Pole Ozbak, Babarud, Aghjalu Sofla, Yalghoz Aghaj, Keshtiban, Pole Bahramlu, and Nezam Abad, which are the final ones before the water reaches Lake Urmia, and no further water is collected beyond these points (see Fig. 1).

The Urmia Lake basin contains 228 rain gauge stations and 16 hydrometer stations. In this research, 16 selected stations leading to Lake Urmia were used. The characteristics of the selected stations for rainfall and discharge in the study basin are presented in Table I.

2.2 Equivalent rainfall computed via the Thyssen polygons

Thiessen polygons, also known as Voronoi cells (Aurenhammer et al., 2013), are utilized to identify the respective rainfall polygon for the surface. These polygons are employed to calculate the rainfall

Table I. Characteristics of the studied stations in the Urmia Lake basin.

Station	River	Average rainfall (mm)
Akhula	Aji chai	235.7
Daryan	Daryan chai	341
Pole Senikh	Senikh chai	203.9
Ghermez gol	Azarshahr chai	355
Khormazard	Mahpari chai	307.1
Shishvan	Ghale chai	276.9
Shirin kandi	Leilan chai	307.1
Gheshlagh Amir	Mordagh chai	345.7
Miandoab	Simine Rud	358.4
Babarud	Barandoz chai	363.1
Keshtiban	Shar chai	315.3
Pole Ozbak	Roze chai	263
Abajalu Sofla	Nazlo chai	270.3
Yalghoz Aghaj	Zola chai	171
Nezam Abad	Zarine Rud	258.7
Pole Bahramlu	Godar chai	251.6

weight for each rain gauge (r_i). They also aid in determining the equivalent rainfall polygon for the area (A_i), enabling the weighing of the rainfall measurements from each rain gauge ($r_i[t]$). Then, the equivalent area-weighted rain is obtained as

$$r_{th}(t) = \frac{\sum_{i=1}^{n} r_i(t) \cdot A_i}{\sum_{i=1}^{n} A_i} \quad (1)$$

The GIS software used to describe the geographic parameters of the watershed is typically used to compute Eq. (1). As shown in Figure 2, the relevant Thiessen polygons were generated with Quantum GIS 0.8 (www.qgis.org) (Shekar and Xiong, 2007; Petrasova et al., 2015), and the equivalent rainfall was calculated with Eq. (1).

2.3 Theory

2.3.1 The Random Forest (RF) model

RF is a machine-learning model based on decision trees. It has been widely employed for solving classification and regression tasks. In this study, the RF algorithm is used as a regression approach to construct a predictive model for a continuous variable. The RF regression technique generates *n* data sets of random samples from the original data set using bootstrapping. The new datasets are then used to build *n* trees, ensuring that each boosted tree in the model is generated using a random subset. As a result, *n* trees (number of trees), N features (number of random predictors used at each node to construct each tree), and tree depth (number of nodes in each tree) act as hyperparameters that optimize the achieved model using a grid search approach that currently ranks all possible RF models using the OOB score. In RF modeling, three parameters require definition: (1) the number of trees to be grown in the forest (n_{tree}), which is a crucial parameter for RF; (2) the number of predictor variables randomly chosen at each node (m_{try}), and (3) the minimum number of observations needed at the terminal nodes of the trees (node size) (refer to Fig. 3).

2.3.2 Boosted-Tree (BT) model

The BT approach is part of a larger class of stochastic grade boosting algorithms comprehended as Tree Net (TM Salford Systems,) and MART (TM Jerill). Recently, this approach has emerged as a highly effective tool for data mining and predictive modeling. These robust algorithms are capable of handling both regression and classification tasks involving continuous and categorical variables (Friedman et al., 2013). The BT approach has been widely used for solving regression problems, particularly for predicting continuous dependent variables. However, when dealing with a large number of classes, the analysis of categorical dependent variables can become less accurate due to the potential need for significant effort and time. Similar to the RF

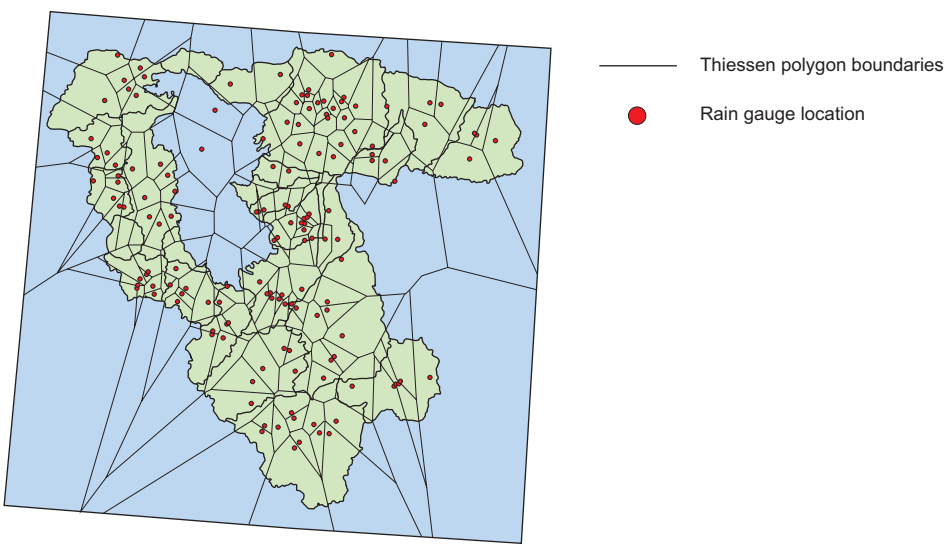

Fig. 2. Thiessen polygon partitioning of the eastern Lake Urmia basin.

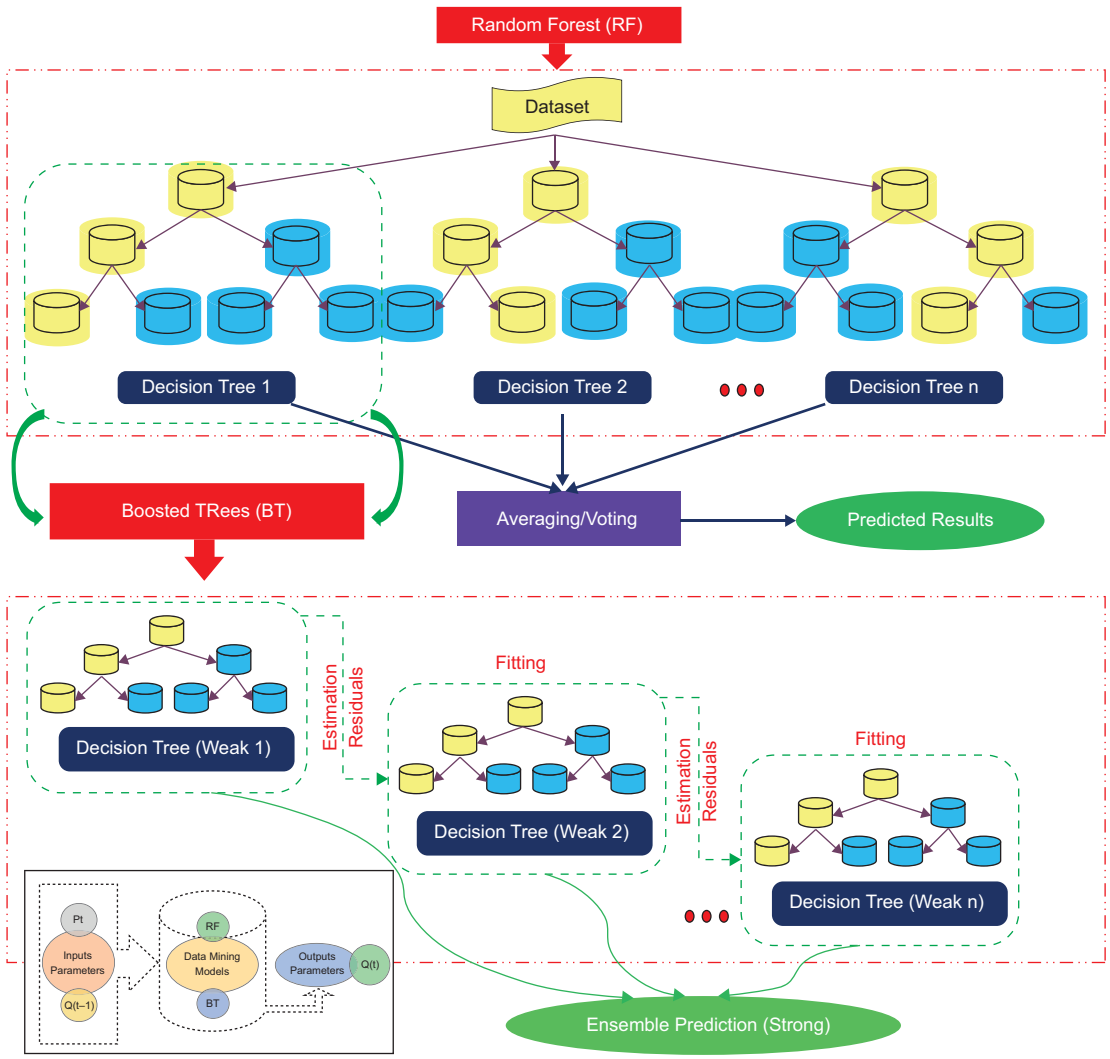

Fig. 3. Structure of the Random Forest and Boosted Tree models, including input and output variables.

algorithm, the BT algorithm is an ensemble learning approach that considers the performance of previous classifiers for classification and regression tasks. In the case of regression, BTs are developed from prediction residuals of the previous tree, and the basic concept is to create a set of simple trees. However, as the complexity of the trees increases, there may be issues with overfitting, where the algorithm builds a model that is overly specialized to the input data. This can be a consideration when using BT techniques in regression problems.

Both the RF and BT algorithms employ an ensemble learning strategy by constructing multiple decision trees. The RF method randomly selects data from the input dataset to build individual decision trees, which are then aggregated to form the final model, with tree weights determined based on performance (Breiman, 2001). Conversely, the BT approach also selects random data from the input dataset, similar to RF, but constructs a BT by iteratively building trees that correct the errors of the previous ones, thereby enhancing model accuracy (Naghibi et al., 2016; Tan et al., 2016). RF and BT differ in how they incorporate the classification history of previous iterations during the sample extraction and model development process. Figure 3 outlines the general algorithms of RF and BT, along with the methodology flowchart.

The analysis and modeling of rainfall-runoff relationships used monthly data from 228 stations inside and outside the Urmia Lake basin, along with monthly flow data from 16 hydrometric stations surrounding the lake. Three input scenarios were created to evaluate the impact of time lags and past rainfall-runoff relationships on forecast performance: (1) current monthly flow from 13 tributaries of Lake Urmia and 16 hydrological stations in the sub-basins; (2) monthly discharge data from the 16 stations between the current month (t) and the previous month (t-1). The optimal time lag for predicting the rain-runoff model, considered the most sensitive parameter, was determined through trial and error. The dataset was divided into 70% test data and 30% validation data for each model, with random selection for training and testing. Data processing methods are detailed in Figure 3. RF and BT models were compared using different runoff and rainfall data combinations, with runoff as the target variable and rainfall as the predictor variable. Inputs included previous monthly runoff (Q_{t-1}) and rainfall (P_t) values, while the output represented current runoff data (Q_t). Various input combinations were evaluated, and both RF and BT models were used to identify the optimal combination (as depicted in Table II and Fig. 4). Using the modeling, the amount of current runoff was obtained with current rainfall and previous runoff. The time lag exists because the model, in addition to the current data, also pays attention to the past data to increase the accuracy of the prediction. In this study, the following hyper-parameters were used for the RF and BT models:

- RF: The model was configured with 200 trees and a maximum tree depth of 10 to prevent overfitting. The minimum number of samples required to split a node was set to five, and at least two samples were required for a leaf node. Additionally, the number of features considered for each split was set to the square root of the total features, and bootstrap sampling was enabled.
- BT: For the BT model, 300 boosting rounds were used, with a learning rate of 0.1 to balance model accuracy and training speed. The maximum depth of each tree was set to five, with a minimum of 10 samples required to split a node. A subsample ratio of 0.8 was used to control overfitting, and the model utilized 80% of the features for each tree.

Rainfall and flow data from 1976 to 2019 were collected and used as training and validation data for these data mining methods. The models were applied using the statistical tool Statistica 12, ArcGis 10.3, Matlab 2021, and Grapher 20.2 to draw graphs. The Iran Meteorological Organization and the Regional Water Company of East and West Azerbaijan provided the necessary parameters for analyzing the relationship between rainfall and runoff in this study. Subsequently, the RF and BT models were implemented, and the results were compared. The rainfall-runoff connection was studied in the following ways: (1) information was collected, associated parameters were collected and calculated; (2) spatial datasets were constructed in raster format; (3) the RF

Table II. Input combination of runoff (Q) and rainfall (P) data.

No	Model	Input	Output
1	RF	P_t, Q_{t-1}	Q_t
2	BT	P_t, Q_{t-1}	Q_t

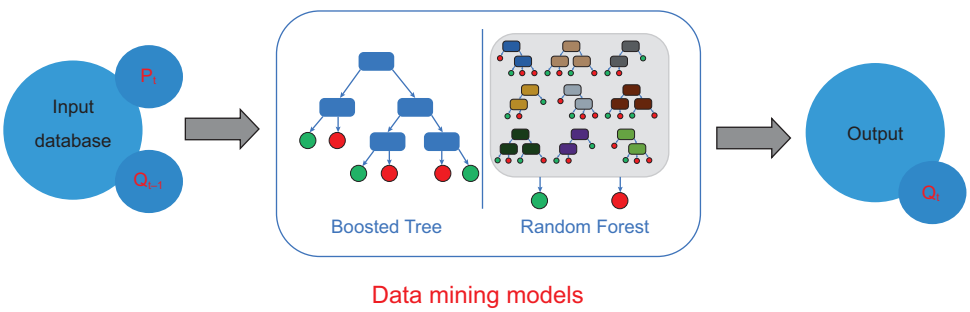

Fig. 4. Research process flow chart.

and BT models were utilized to study the relationship between rainfall and runoff, and the significance values of each predictor were computed during the course of the study; and (4) The rainfall-runoff data were used to validate the susceptibility from 1976.

2.4 Performance criteria

The performance of the RF and BT approaches was evaluated using various criteria, which included root mean square error (RMSE), Pearson correlation coefficient (r), determination coefficient (R^2), and Nash-Sutcliffe efficiency (NSE) (Lan, 2014). The R^2 value was utilized to measure the linear relationship between observed and estimated rain and runoff amounts, with values exceeding 1 indicating superior prediction and 1 representing excellent prediction. The RMSE assessed the goodness of fit for high rainfall-runoff values, with lower RMSE values indicating better forecast performance and a value of 0 suggesting excellent prediction (Hamidi et al., 2015). Moreover, the efficiency coefficient was employed to compare the variability of observed rainfall and runoff values with the differences between observed and estimated values. In this research, cross-correlation (CC), R^2, NSE, and RMSE are widely used in hydrological modeling to assess model performance from different perspectives. Together, these metrics provide a comprehensive evaluation of the model's accuracy.

RMSE: due to its sensitivity to outliers in the data set, this measure may be prone to errors when simulating high flow rates (Dawson et al., 2006):

$$RMSE = \sqrt{\frac{\sum_{i=1}^{n}(P_i - O_i)^2}{n}} \tag{2}$$

Pearson correlation coefficient (r):

$$r = \frac{n(\sum_{i=1}^{n} O_i . P_i) - (\sum_{i=1}^{n} O_i).(\sum_{i=1}^{n} P_i)}{\sqrt{(n\sum_{i=1}^{n} O_i^2) - (\sum_{i=1}^{n} O_i)^2).(n\sum_{i=1}^{n} P_i^2) - (\sum_{i=1}^{n} P_i)^2)}} \tag{3}$$

R-squared (R^2): the strength of the relationship between the observed and simulated time series is quantified by the coefficient of determination (R^2), which ranges from 0.0 to 1.0, with larger values indicating greater collinearity.

$$R^2 = \frac{\left[\sum_{i=1}^{n}\left(O_i - \bar{O}_i\right).\left(P_i - \bar{P}_i\right)\right]^2}{\sum_{i=1}^{n}\left(O_i - \bar{O}_i\right).\sum_{i=1}^{n}\left(P_i - \bar{P}_i\right)} \tag{4}$$

Nash-Sutcliffe efficiency (NSE): In the scenario of a perfect model with zero estimation error variance, the resulting Nash-Sutcliffe efficiency is equals to 1 (NSE = 1):

$$NSE = 1 - \frac{\sum_{i=1}^{n}(P_i - O_i)^2}{\sum_{i=1}^{n}(P_i - \bar{P})^2} \tag{5}$$

where P_i and Q_i represent the observed and modelled runoff using the developed models, respectively, while O_i is the average of observed runoff, and n is number of observations.

Trend analysis, a crucial tool for assessing climate change, utilizes various methods categorized as parametric and non-parametric. While parametric tests are considered stronger in normally distributed data, non-parametric tests, such as the Mann-Kendall method, are preferable for non-normal data conditions, common in climate series like rainfall and streamflow (Pasquini, 2006; Sabouhi and Soltani, 2008). Originally proposed by Mann (1945) and further developed by Kendall (1975), the Mann-Kendall test is extensively used in hydrological and meteorological time series analysis (Lettenmaier et al., 1994; Serrano et al., 1999). Its advantages include applicability to diverse time series distributions and low sensitivity to extreme values (Turgay and Ercan, 2005). The test's null hypothesis assumes randomness and the absence of a trend, while rejecting it indicates the presence of a trend in the data series. The Mann-Kendall test is defined by the statistic S as follows:

$$S = \sum_{i=1}^{n-1}\sum_{j=i+1}^{n} sign\,(Xi + Xj) \tag{6}$$

$$sgn(x) = \begin{cases} +1 & if \quad , (x_j - x_k) > 0 \\ 0 & if \quad , (x_j - x_k) = 0 \\ -1 & if \quad , (x_j - x_k) < 0 \end{cases} \tag{7}$$

where X_j and X_i are the sorted values of the sample, and n is the number of samples.

The variance is calculated with Eqs. (8) or (9).

$$Var\,(S) = \frac{n(n-1)(2n-1) - \sum_{i=1}^{m} t(t-1)(2t+5)}{18} \tag{8}$$

$$Var\,(S) = \frac{n(n-1)\left(2n+5\right)}{18} \tag{9}$$

where n is the number of observation data and m represents the number of series in which there is at least one repeated data. It also represents the frequency of data with the same value.

The standardized score Z and the variance of the statistic S are calculated from the following equation:

$$Zc = \begin{cases} \frac{S-1}{\sqrt{Var\,(s)}} & , S > 0 \\ 0 & , S = 0 \\ \frac{S+1}{\sqrt{Var\,(s)}} & , S < 0 \end{cases} \quad (10)$$

Positive values of Z indicate increasing trends, while negative values of Z indicate decreasing trends. When $S = 0$, there is no significant or non-significant trend in the data. These conditions are rarely ideal for hydrological data. In this study, significance levels of P = 0.05 were employed.

3. Discussion and results

3.1 Results related to the time series of rainfall and runoff for the studied time period

Figures 5 and 6 show the time series data concerning the rainfall and runoff of 16 stations within the east and west regions of the Urmia basin, which align with the results obtained from the Mann-Kendall test for annual rainfall and discharge (Tables II and III). According to Table II, Kendall's statistic for the rainfall variable at stations Akhula, Daryan, Pole Senikh, Shishvan, Gheshlagh Amir, Ghermez Gol, Shirin Kandi, and Khormazad is determined as –0.89, 1.65, 0.031, 0.77, –1.15, 1.61, –0.41 and 1.30, respectively. Similarly, the values obtained in the west sub-basin stations Miandoab, Babarud, Keshtiban, Pole Ozabk, Yalghoz Aghaj, Nezam Abad, and Pole Bahramlo are 1.18, 0.39, –2.61, –1.79, 1.13, –0.39, 0.94 and –1.42, respectively. The results indicate that annual rainfall in the period 1976-2019 is not statistically significant at the 95% level for all stations. Therefore, it can be inferred that annual rainfall at these stations during the above-mentioned period has shown no significant trend, with natural variations occurring during this period. The data exhibit oscillatory behavior, with some years showing increasing trends and others showing decreasing trends.

In addition to rainfall, the results obtained from the Mann-Kendall test indicate that the discharge from stations in both the eastern and western sub-basins of Lake Urmia exhibits a decreasing trend. In recent years, a considerable reduction in the discharge trend has been observed, posing a significant threat to Lake Urmia. Table III shows the discharge variables for eastern stations Akhula, Daryan, Pole Senikh, Shishvan, Gheshlagh Amir, Ghermez Gol, Shirin Kandi, and Khormazard, determined as –2.369, –0.35, –2.264, –1.1, –2.19, –1.82, –1.6, and –1.2, respectively. Similarly, the values obtained in the west sub-basin (Table IV) for stations Miandoab, Babarud, Keshtiban, Pole Ozabk, Yalghoz Aghaj, Nezam Abad, and Pole Bahramlo, are –2.61, –3.52, –2.75, –1.6, –2.63, –1.1, –0.69 and –0.69, respectively, indicating a statistically significant decreasing trend at the 95% confidence level. According to the results obtained from Tables III and IV, and the graphs in Figures 5 and 6, the inflow discharge into Lake Urmia has decreased at all stations during recent years, which is consistent with findings from other research and studies on the lake basin and is considered the primary reason for its declining water level (Vaheddoustand Aksoy, 2018; Hamidi-Razi et al., 2019; Lari et al., 2019).

For further comparison, Figures 5 and 6 show the time series of the observed rainfall and runoff data at 16 stations over this period (1976-2019). In these charts, it can be seen that in each station, the temporal trend of rainfall shows the frequency of yearly rainfall and that in some years, it has irregularly decreased and sometimes increased. In their study's results, Salehi et al. (2018) confirmed that the frequency of monthly rainfall events lower than 5 mm increased significantly at a 1% level in certain areas while showing no significant trend in other areas. Additionally, the area with rainfall events in the range of 10-15 mm exhibited a significant decreasing trend. Furthermore, the direction of the runoff series in the studied stations situated in the eastern and western parts of Lake Urmia showed a decreasing trend in discharge changes. Runoff figures indicate a complete decrease in lake inflow over the past 43 years, notably declining in recent years. In fact, Figures 5 and 6 confirm the results of the Mann-Kendall test presented in Tables II and III.

This decline is primarily attributed to increased local water demand and intensive agricultural development, accounting for over 60% of renewable water resource usage and 93% of total water resource

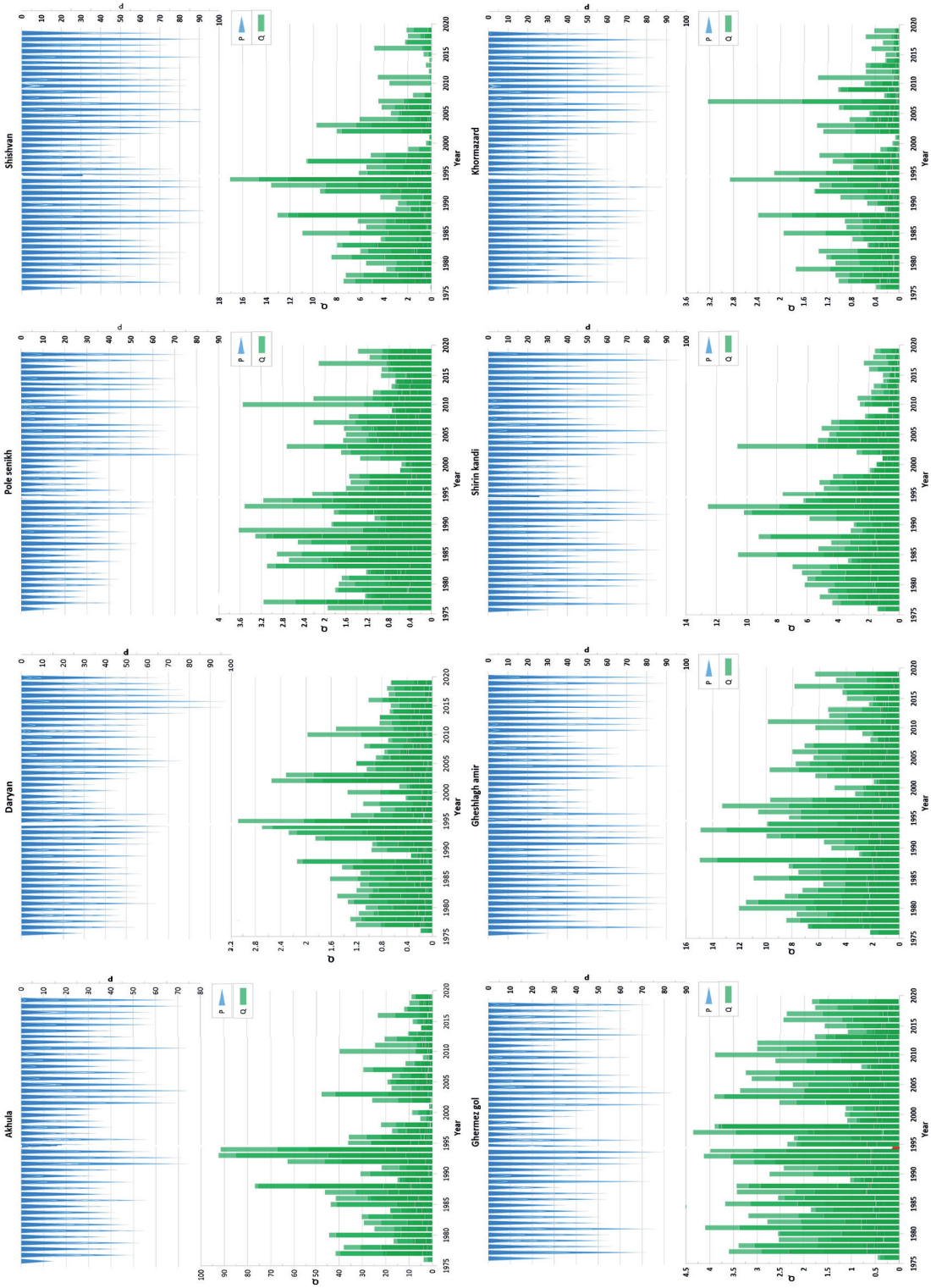

Fig. 5. Time-series plots of observed rainfall and runoff values at eight stations in the eastern sub-basin (1976-2019).

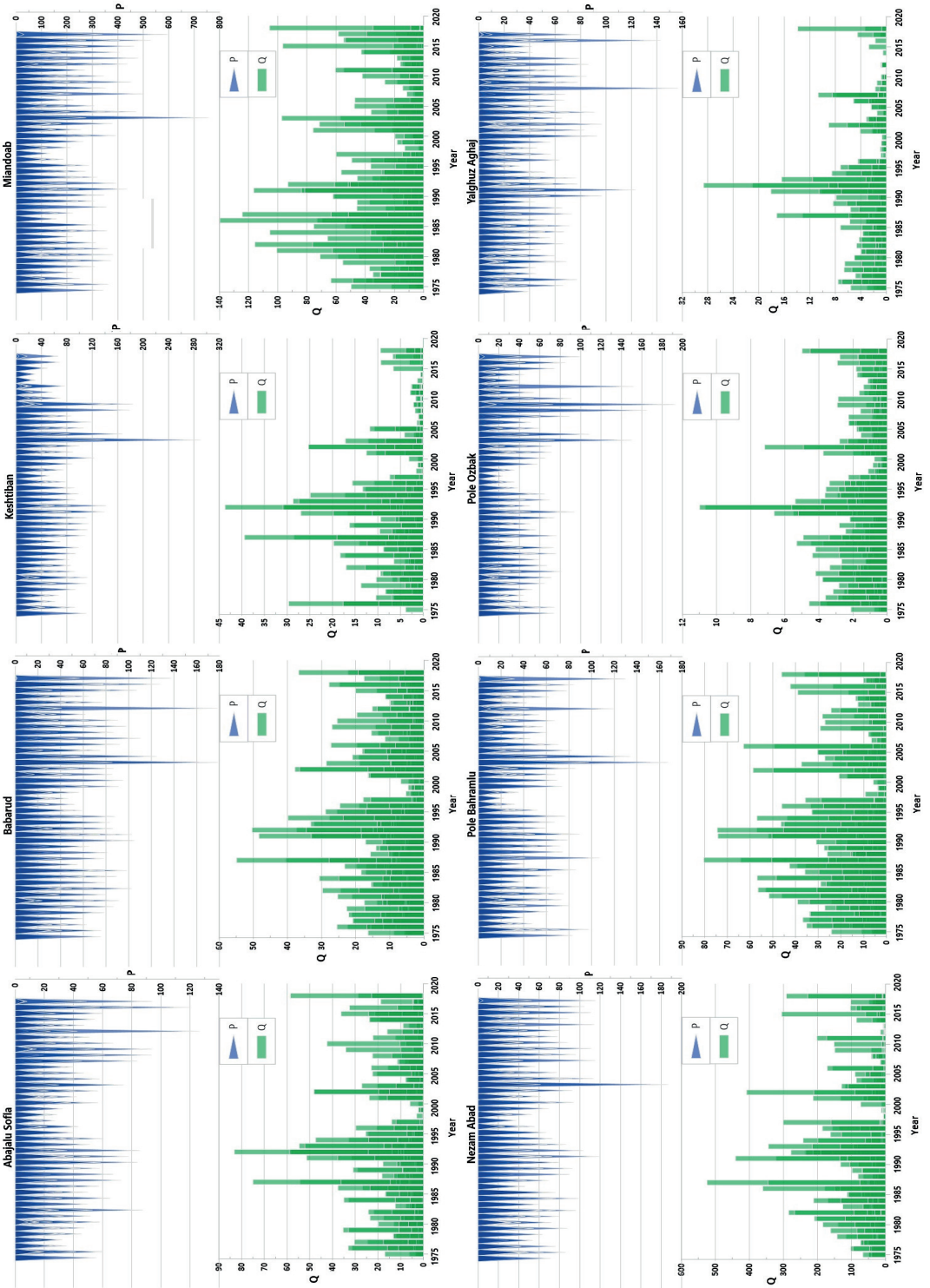

Fig. 6. Time-series plots of observed rainfall and runoff values at eight stations in the western sub-basin (1976-2019).

Table III. Statistical values of the Mann-Kendall test for rainfall and runoff in the eastern sub-basin (1976-2019).

State	Station	Rainfall	Runoff
East Azarbaijan	Akhula	–0.89	–2.369
	Daryan	1.65	–0.35
	Pole senikh	0.031	–2.264
	Shishvan	0.77	–1.1
	Gheshlagh amir	–1.15	–2.19
	Ghermez gol	1.61	–1.82
	Shirin kandi	–0.41	–1.6
	Khormazard	1.30	–1.2

Table IV. Statistical values of the Mann-Kendall test for rainfall and runoff in the western sub-basin (1976-2019).

State	Station	Rainfall	Runoff
West Azarbaijan	Miandoab	1.18	–2.61
	Babarod	0.39	–3.52
	Keshtiban	–2.61	–2.75
	Pole Ozbak	–1.79	–1.6
	Abajalo Sofla	1.13	–2.63
	Yalghoz Aghaj	–0.39	–1.1
	Nezam Abad	0.94	–0.69
	Pole Bahramlo	–1.42	–0.69

utilization in the basin (Nordberg et al., 2014). According to the findings of Nazeri-Tahroudi et al. (2018), the decreasing trend in the water level of Lake Urmia was observed one year after the declining trend in the flow data. Numerous studies have been carried out to investigate trends in river flow and rainfall in the Lake Urmia basin, and all of them have confirmed that not only the water inflow to the lake has decreased, but also the water level has declined. The significant loss of water at Lake Urmia can be attributed to several factors, including: (1) construction of dams on the 13 rivers that flow into the lake, which has resulted in reduced inflows and contributed to the lowering of the lake's water level; (2) increased groundwater pumping; (3) water diversions; (4) climate change, and (5) drought (Ahmadaali et al., 2018; Vaheddoost and Aksoy, 2018; Alizade et al., 2019; Hamidi-Razi et al., 2019; Lari et al., 2019; Marks, 2019; Bashirian et al., 2020; Hosseini-Moghari et al., 2020; Javadzadeh et al., 2020). It should be noted that in Figures 5 and 6, the unit of runoff is $m^3 s^{-1}$, and the unit of rainfall is mm.

To study the selected rainfall and runoff stations in the mentioned period, the rainfall and runoff statistics (average, minimum, maximum) for these years are presented in Tables V and VI, which were divided into five columns, and subsequently, the third, fourth, and fifth columns were segregated into two distinct categories or sections. The third column (total data) contains the P and Q parts. The fourth and fifth columns display the allocation of data into two separate sets: the training set and the test set. Consequently, the BT and RF models were trained and tested using real data in this study. As shown in Tables V and VI in the "total data" column, the Shishvan and Miandoab stations have the highest average rainfall. Similarly, the Akhula and Miandoab stations have the highest average runoff among the recorded events, making them the most influential in affecting the water volume of Lake Urmia. Conversely, the Pole Senikh and Abajalu Sofla stations registered the lowest average rainfall, while the Khormazard and Pole Ozbak stations showed the lowest average runoff in the study area.

In this section, the validation process of the optimal BT and RF models is presented to showcase their ability to model the rainfall-runoff relationship. Tables VII and VIII present the validation statistics of each optimal model for all stations over the eastern and western sub-basins of Urmia Lake in the period (1976-2019).

To select the best model for each station in the basin of Lake Urmia, statistical analyses were also performed to determine the cross-correlation between rainfall-runoff and past runoff at each station. R^2, NSE, and RMSE statistics were used to evaluate this cross-correlation . The results indicated that both RF and BT models performed well in both east and west sub-basins. However, as seen in Table VII, the BT model outperformed the RF model in rainfall-runoff modeling at five out of the eight studied stations in the eastern sub-basin, while the RF model performed better at three stations. Overall, a strong correlation between rainfall and runoff parameters was observed across all stations. As outlined in Table VII, the maximum cross-correlation in the test dataset for the RF and BT models ranged from 0.71 to 0.82. The optimal model for each station varied depending on the specific characteristics of that station.

On the other hand, as shown in Table VIII, the RF model outperformed the BT model in rainfall-runoff

Table V. Statistics parameters of rainfall and runoff data and Random Forest (RF) and Boosted Tree (BT) models at eastern stations (1976-2019).

Station	Parameter	Whole data set		Training set		Test set	
		P (mm month^{-1})	Q (m^3 s^{-1})	BT	RF	BT	RF
Akhula	Mean	22.22	7.90	7.68	8.29	7.49	6.32
	Minimum	0.00	0.00	0.00	0.00	0.00	0.00
	Maximum	77.66	92.50	76.85	76.85	46.29	47.47
Daryan	Mean	25.11	0.40	0.41	0.43	0.38	0.33
	Minimum	0.00	0.00	0.00	0.00	0.00	0.00
	Maximum	97.19	3.07	3.24	3.24	2.55	2.32
Pole Senikh	Mean	19.78	0.66	0.66	0.70	0.68	0.61
	Minimum	0.00	0.00	0.00	0.00	0.00	0.00
	Maximum	81.25	3.63	3.63	3.86	3.86	3.70
Shishvan	Mean	30.03	1.21	1.29	1.54	1.33	0.83
	Minimum	0.00	0.00	0.00	0.00	0.00	0.00
	Maximum	98.70	17.08	32.94	32.94	10.97	9.69
Gheshlagh Amir	Mean	26.38	2.16	2.09	2.32	2.33	1.83
	Minimum	0.00	0.01	1.01	0.01	0.01	0.01
	Maximum	91.69	14.97	14.97	14.97	13.30	10.60
Ghermez Gol	Mean	23.32	0.81	0.82	0.86	0.81	0.73
	Minimum	0.00	0.00	0.00	0.00	0.00	0.00
	Maximum	88.03	4.35	4.12	4.35	4.35	3.75
Shirin Kandi	Mean	26.69	1.45	1.41	1.61	1.63	1.20
	Minimum	0.00	0.00	0.00	0.00	0.00	0.00
	Maximum	96.73	12.54	12.56	16.72	16.72	10.20
Khormazard	Mean	26.68	0.25	0.25	0.29	0.26	0.18
	Minimum	0.00	0.00	0.00	0.00	0.00	0.00
	Maximum	94.18	14.81	3.23	3.23	1.94	1.40

modeling at five out of the eight studied stations in the western sub-basin, while the BT model performed better at three stations. As seen in Table VIII, the maximum cross-correlation in the test dataset for the RF and BT models ranged from 0.72 to 0.88. Overall, a strong correlation between rainfall and runoff parameters was observed across all stations in this sub-basin.

In the Akhula station, a statistical analysis comparing the RF and BT models revealed that the former exhibited higher modeling accuracy. In this station, RF yielded a CC of 0.85, R^2 of 0.73, NSE of 0.72, and RMSE of 6.77 on the training dataset, and CC = 0.82, R^2 = 0.67, NSE = 0.66, and RMSE = 5.43 on the test dataset. Conversely, at the Daryan station, RF yielded CC = 0.87, R^2 = 0.76, NSE = 0.75, and RMSE = 0.27 on the training dataset, and CC = 0.80, R^2 = 0.64, NSE = 0.63, and RMSE = 0.22 on the test dataset. At the Pole Senikh station, the CC, R^2, NSE, and RMSE results on the training dataset for BT model were 0.81, 0.66, 0.66, and 0.41, respectively, and 0.77, 0.59, 0.59, and 0.47, respectively, on the testing dataset. Conversely, at the Shishvan station, the BT model outperformed the RF model, with CC values of 0.90 on the training dataset, and 0.75 on the testing dataset, respectively. Similarly, at the Gheshlagh Amir station, the BT model exhibited better performance,

Table VI. Statistics parameters of rainfall and runoff data and Random Forest (RF) and Boosted Tree (BT) models at western stations (1976-2019).

Station	Parameter	Whole data set (1976-2019)		Training set		Test set	
		P (mm month^{-1})	Q (m^3 s^{-1})	BT	RF	BT	RF
Miandoab	Mean	128.99	14.92	14.51	15.84	15.93	13.32
	Minimum	0.00	0.00	0.00	0.00	0.00	0.00
	Maximum	755.95	139.63	115.61	139.63	139.63	116.39
Babarud	Mean	32.30	7.29	7.00	7.26	7.99	7.38
	Minimum	0.00	0.00	0.00	0.00	0.00	0.00
	Maximum	178.52	54.86	54.86	54.86	55.33	37.24
Keshtiban	Mean	39.62	3.07	2.86	3.08	3.56	3.06
	Minimum	0.00	0.00	0.00	0.00	0.00	0.00
	Maximum	290.27	43.65	39.36	43.65	43.65	30.51
Pole Ozbak	Mean	25.10	1.04	0.98	1.05	1.18	1.01
	Minimum	0.00	0.00	0.00	0.00	0.00	0.00
	Maximum	192.57	10.98	6.62	10.98	10.98	10.64
Abajalu Sofla	Mean	22.96	6.65	6.41	6.52	7.27	6.97
	Minimum	0.00	0.00	0.00	0.00	0.00	0.00
	Maximum	126.28	83.12	74.94	83.12	83.12	58.52
Yalghoz Aghaj	Mean	27.02	1.48	1.30	1.46	1.88	1.52
	Minimum	0.00	0.00	0.00	0.00	0.00	0.00
	Maximum	156.41	28.62	18.07	28.62	28.62	20.96
Nezam Abad	Mean	32.97	41.89	39.09	43.30	48.20	38.94
	Minimum	0.00	0.00	0.10	0.04	0.01	0.01
	Maximum	186.96	523.92	440.58	523.92	523.92	320.99
Pole Bahramlu	Mean	25.69	9.55	9.06	9.52	10.75	9.67
	Minimum	0.00	0.00	0.00	0.00	0.00	0.00
	Maximum	167.52	80.31	80.31	80.31	74.37	62.88

with CC values of 0.86 on the training dataset and 0.80 on the testing dataset, respectively. Also, at the Ghermez Gol station, the RF model performed better than BT, achieving a CC = 0.91, R^2 = 0.82, NSE = 0.82, and RMSE = 0.41 on the training dataset, and CC = 0.84, R^2 = 0.70, NSE = 0.69, and RMSE = 0.48 on the testing dataset. At the Shirin Kandi station, the BT model outperformed the RF model, with CC values of 0.85 on the training dataset and 0.77 on the testing dataset, respectively. Similarly, at the Khormazard station, the BT model demonstrated a stronger relationship between rainfall and runoff compared to the RF model. The CC values were 0.73 on the training dataset and 0.71 on the testing dataset, respectively.

Notably, in the Akhula station, the BT model exhibited higher CC coefficients in the training data compared to the RF model. However, this higher performance in training data did not translate to better accuracy in the test dataset, suggesting overfitting. Consequently, the RF model, which performed well in both training and testing, was selected as the superior model. Conversely, at the Gheshlagh Amir, Shirin Kandi, and Khormazard stations, the RF model was overfitted, leading to inferior performance compared to BT, thus making this model the preferred choice.

Table VII. Performance of the Random Forest (RF) and Boosted Tree (BT) models in the training and testing sets over the eastern sub-basin (1976-2019).

Station	Whole data set	CC		R2		NSE		RMSE	
		BT	RF	BT	RF	BT	RF	BT	RF
Akhula	Train	0.87	0.85	0.76	0.73	0.76	0.72	6.10	6.77
	Test	0.81	0.82	0.65	0.67	0.65	0.66	6.05	5.43
Daryan	Train	0.87	0.87	0.75	0.76	0.75	0.75	0.26	0.27
	Test	0.78	0.80	0.61	0.64	0.61	0.63	0.28	0.22
Pole Senikh	Train	0.81	0.80	0.66	0.64	0.66	0.63	0.41	0.45
	Test	0.77	0.66	0.59	0.44	0.59	0.44	0.47	0.50
Shishvan	Train	0.90	0.81	0.82	0.65	0.79	0.53	1.53	2.49
	Test	0.75	0.70	0.56	0.48	0.51	0.44	1.66	1.23
Gheshlagh Amir	Train	0.86	0.90	0.74	0.81	0.74	0.80	1.31	1.26
	Test	0.80	0.77	0.64	0.60	0.64	0.58	1.70	1.37
Ghermez Gol	Train	0.87	0.91	0.76	0.82	0.76	0.82	0.44	0.41
	Test	0.74	0.84	0.54	0.70	0.54	0.69	0.65	0.48
Shirin Kandi	Train	0.85	0.87	0.72	0.76	0.72	0.75	0.98	1.09
	Test	0.77	0.63	0.59	0.40	0.59	0.26	1.45	1.32
Khormazard	Train	0.73	0.79	0.54	0.62	0.53	0.62	0.27	0.28
	Test	0.71	0.69	0.51	0.48	0.51	0.36	0.26	0.18

CC: cross-correlation; R2: determination coefficient; NSE: Nash-Sutcliffe efficiency; RMSE: root mean square error.

Table VIII. Performance of the Random Forest (RF) and Boosted Tree (BT) models in the training and testing sets over the western sub-basin (1976-2019).

Station	Whole data set	CC		R^2		NSE		RMSE	
		BT	RF	BT	RF	BT	BT	RF	BT
Miandoab	Train	0.83	0.86	0.68	0.73	0.68	0.72	11.54	11.98
	Test	0.82	0.85	0.68	0.71	0.68	0.71	13.74	10.49
Babarud	Train	0.89	0.90	0.79	0.80	0.86	0.78	3.96	4.09
	Test	0.87	0.87	0.76	0.76	0.77	0.76	4.75	4.10
Keshtiban	Train	0.83	0.87	0.83	0.75	0.75	0.73	2.82	3.06
	Test	0.82	0.74	0.82	0.54	0.65	0.51	4.15	3.75
Pole Ozbak	Train	0.88	0.87	0.78	0.76	0.88	0.73	0.51	0.68
	Test	0.81	0.81	0.65	0.66	0.64	0.64	1.03	0.79
Abajalu Sofla	Train	0.81	0.83	0.65	0.69	0.74	0.67	6.30	6.97
	Test	0.78	0.83	0.61	0.69	0.61	0.67	8.33	6.57
Yalghoz Aghaj	Train	0.82	0.76	0.67	0.57	0.75	0.52	1.30	1.98
	Test	0.72	0.65	0.51	0.42	0.45	0.41	2.79	2.14
Nezam Abad	Train	0.81	0.87	0.66	0.76	0.73	0.73	36.59	38.18
	Test	0.81	0.84	0.66	0.70	0.61	0.69	51.74	32.91
Pole Bahramlu	Train	0.86	0.93	0.74	0.86	0.82	0.85	6.69	5.60
	Test	0.88	0.88	0.77	0.77	0.75	0.77	8.03	6.54

CC: cross-correlation; R^2: determination coefficient; NSE: Nash-Sutcliffe efficiency; RMSE: root mean square error.

On the other hand, Table VIII shows that at the Miandoab station, the RF model exhibited higher accuracy in modeling compared to BT. In this station, RF achieved a CC of 0.86, R^2 of 0.73, NSE of 0.72, and RMSE of 11.98 on the training dataset, and CC = 0.85, R^2 = 0.71, NSE = 0.71, and RMSE = 10.49 on the test dataset. Conversely, at the Babarud station, BT yielded a CC = 0.89, R^2 = 0.79, NSE = 0.86, and RMSE = 3.96 on the training dataset, and CC = 0.87, R^2 = 0.76, NSE = 0.77, and RMSE = 4.75 on the test dataset. At the Keshtiban station, the CC, R^2, NSE, and RMSE results on the training dataset for the BT model were 0.83, 0.83, 0.75 and 2.82, respectively, and 0.82, 0.82, 0.65, and 4.15, respectively, on the testing dataset. Also, at the Pole Ozbak station, the RF model outperformed the BT model, with CC values of 0.87 on the training dataset, and 0.81 on the testing dataset, respectively. Similarly, at the Abajalu Sofla station, the RF model exhibited better performance, with CC values of 0.83 on the training dataset, and 0.83 on the testing dataset. Also, at the Yalghoz Aghaj station, the BT model performed better than RF, achieving a CC = 0.82, R^2 = 0.67, NSE = 0.75, and RMSE = 1.30 on the training dataset, and CC = 0.72, R^2 = 0.51, NSE = 0.45, and RMSE = 2.79 on the testing dataset. At the Nezam Abad station, the RF model outperformed the BT model, with CC values of 0.87 on the training dataset and 0.84 on the testing dataset. Similarly, at the Pole Bahramlu station, the RF model demonstrated a stronger relationship between rainfall and runoff compared to the BT model. The CC values were 0.93 on the training dataset and 0.88 on the testing dataset.

Notably, in Babarud and Keshtiban stations, the RF model exhibited higher CC coefficients in the training data compared to the BT model. However, this higher performance in training data did not translate to better accuracy in the test dataset, suggesting overfitting. Consequently, the BT model, which performed well in both training and testing, was selected as the superior model. Conversely, at the Pole Ozbak station, the BT model was overfitted, leading to inferior performance compared to RF, thus making the RF model the preferred choice.

For a more thorough comparison, scatter and violin plots of simulated runoff for the period 1976-2019, using RF and BT models based on the testing data sets for the 16 study stations in the Urmia Lake basin, are depicted in Figs. 7 and 8, confirming the results presented in Tables VI and VII. These plots illustrate observed and modeled runoff values with RF and BT models during the study periods. The scatterplots for the RF model for stations Akhula, Daryan, and Ghermez Gol in the eastern sub-basin and Miandoab, Pole Ozbak, Abajalu Sofla, Nezam Abad, and Pole Bahramlu in the western sub-basin, show R^2 values of 0.67, 0.64, 0.70, 0.71, 0.66, 0.69, 0.70, and 0.77, respectively, for the period 1976-2019.

Similarly, the R^2 values for the BT model at Pole Senikh, Shishvan, Gheshlagh Amir, Shirin Kandi and Khormazard stations over the eastern sub-basin were 0.59, 0.56, 0.64, 0.59, and 0.51, respectively, and the R^2 values for the western stations Babarud, Keshtiban, and Yalghoz Aghaj were 0.76, 0.82, and 0.51, respectively. Based on the fit line equations and R^2 values, it can be concluded that the BT model provides the most accurate estimates for the rainfall-runoff relationship. Also, the linear trends were included to provide a simple, interpretable view of the relationship between observed and predicted values, even if R^2 values are less than 0.5. While the models capture non-linear complexities, the linear fits help visualize the overall trend for comparison purposes.

4. Conclusions

This study aimed to enhance rainfall-runoff modeling for 16 key stations in the Urmia Lake basin, Iran. The rainfall and runoff data from 228 rain and 16 runoff gauge stations spanning 43 years (1976-2019) were utilized as hydro-climatic inputs. The objective was to identify the most effective model based on hydrological insights for accurate monthly discharge estimation while considering time lag effects. To achieve this, chronological records of these parameters and regional-scale meteorological inputs were analyzed using heuristic RF and BT methods. Predictor significance for each variable was evaluated, and the RF and BT models were compared. The rainfall-runoff modeling performance of both models for the 16 stations was assessed using training and testing for the whole study period, and the results were compared to determine the best-performing model for each station.

In general, the RF model provided better estimates for the eastern stations Akhula, Daryan, and

Ghermez Gol, with CCs of 0.82, 0.80, and 0.84. However, the BT model outperformed RF for the Pole Senikh, Shishvan, Gheshlagh Amir, Shirin Kandi, and Khormazard stations, with CC values of 0.77, 0.75, 0.80, 0.77, and 0.71, respectively. For the western stations, the RF model yielded better estimates for Miandoab, Pole Ozbak, Abajalu Sofla, Nezam Abad, and Pole Bahramlu stations, with CC values of 0.85, 0.81, 0.83, 0.84, and 0.88, respectively. Conversely, the BT model performed better for Babarud, Keshtiban, and Yalghoz Aghaj stations, with CC coefficients of 0.87, 0.82, and 0.72, respectively.

However, the results obtained from these models prove their effectiveness in providing valuable insights for hydrological applications, particularly in rainfall-runoff estimation. A time series analysis of the stations revealed irregular fluctuations in monthly rainfall, with some years showing decreases and others showing increases. Additionally, the runoff trend across the stations indicated a general decrease over time, although some fluctuations were observed. Notably, after 1995, there was a notable increase in the discharge trend. These findings highlight a significant decrease in inflow to Lake Urmia over the past 43 years, with a particularly sharp decline in

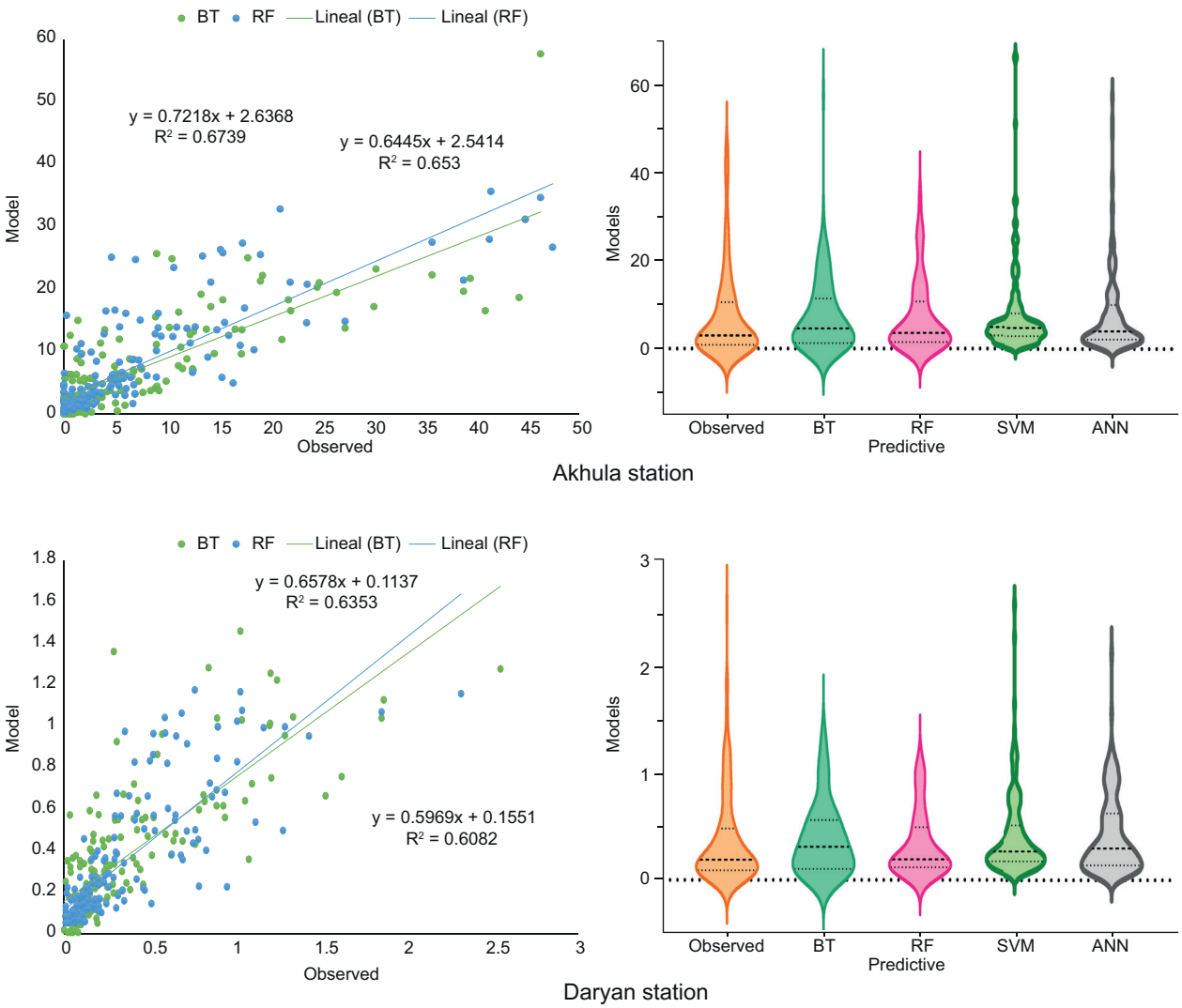

Fig. 7. Verification scatter plots and violin plots of simulated runoff using the Random Forest (RF) and Boosted Tree (BT) models in the eastern sub-basin.

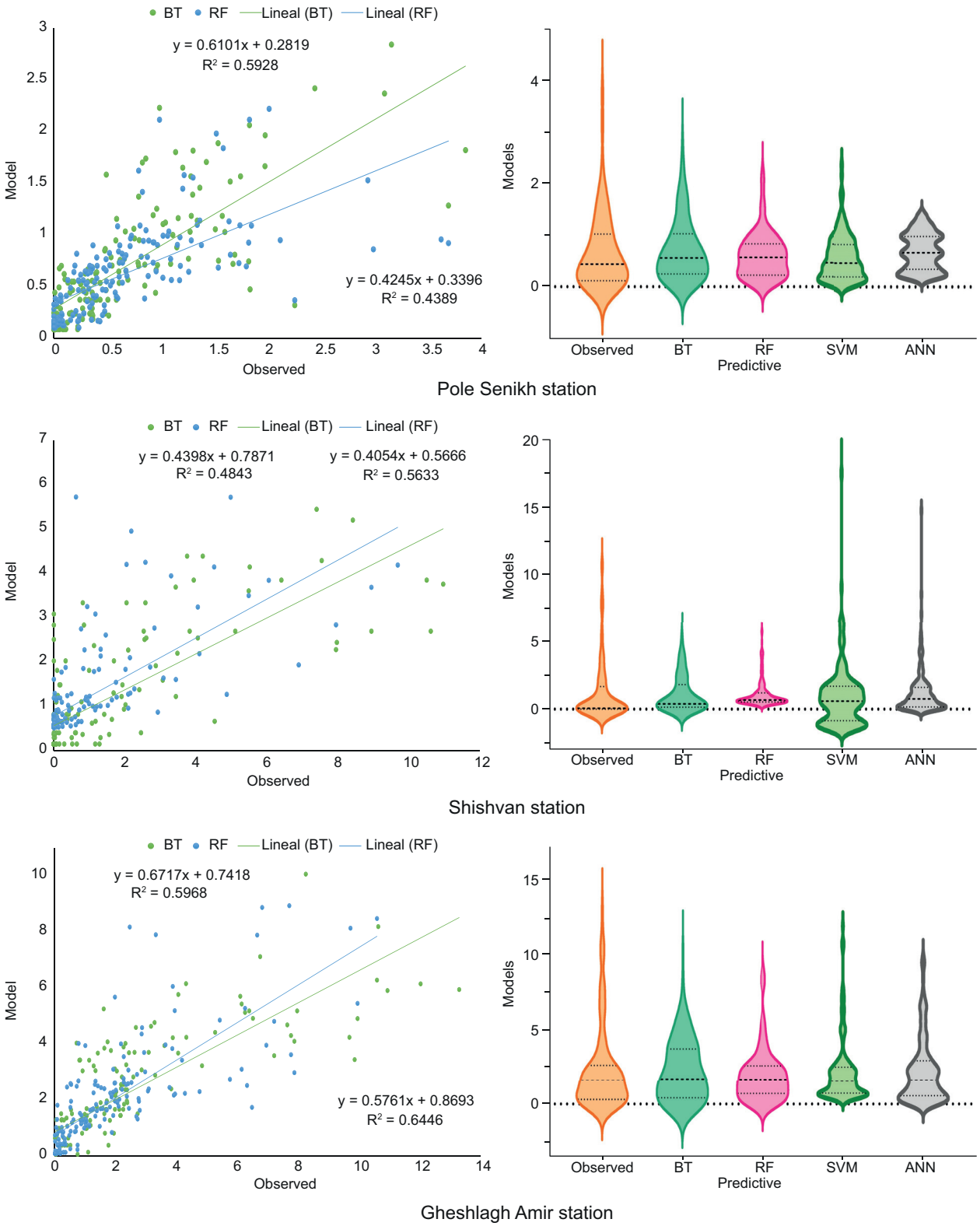

Fig. 7. Verification scatter plots and violin plots of simulated runoff using the Random Forest (RF) and Boosted Tree (BT) models in the eastern sub-basin.

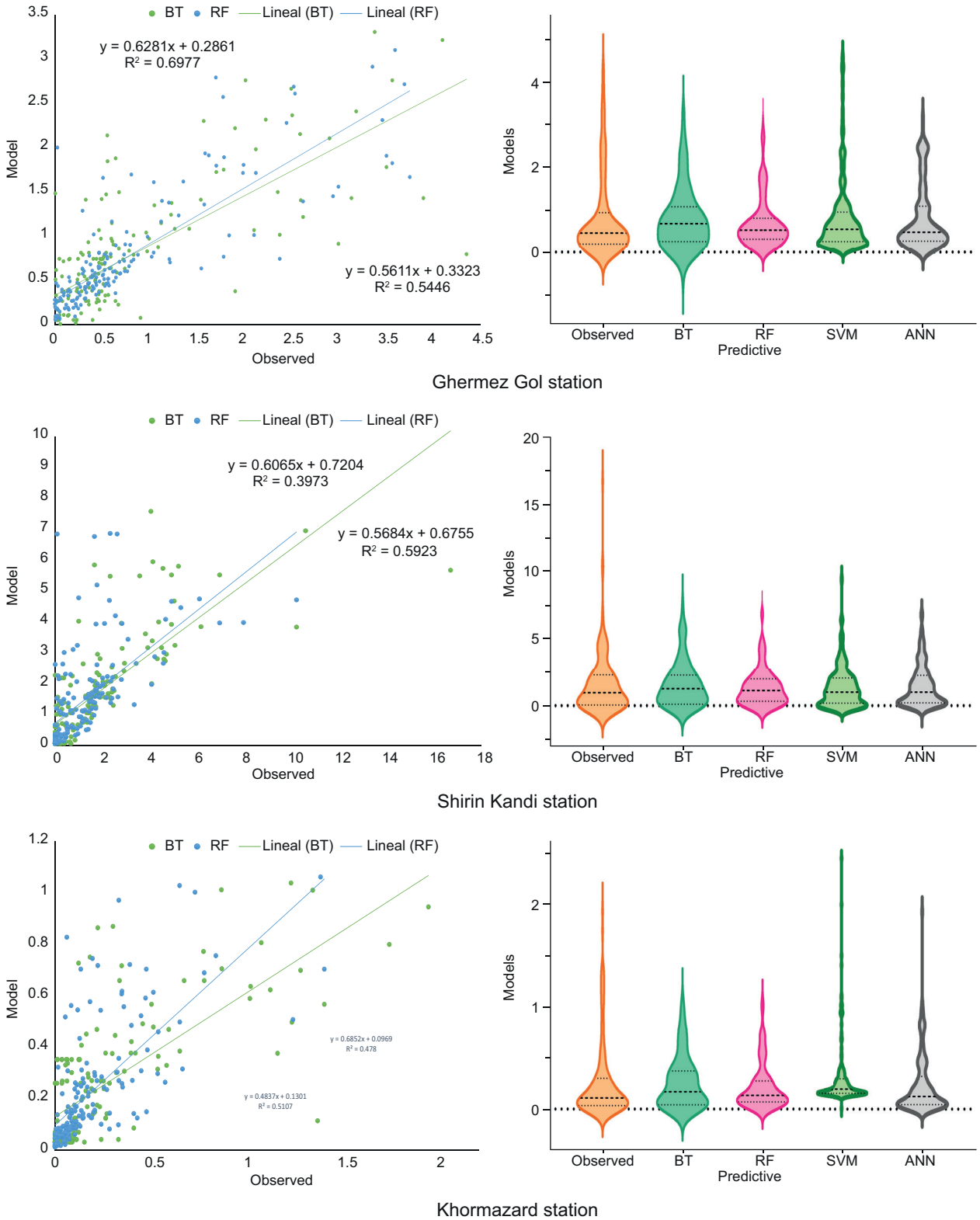

Fig. 7. Verification scatter plots and violin plots of simulated runoff using the Random Forest (RF) and Boosted Tree (BT) models in the eastern sub-basin.

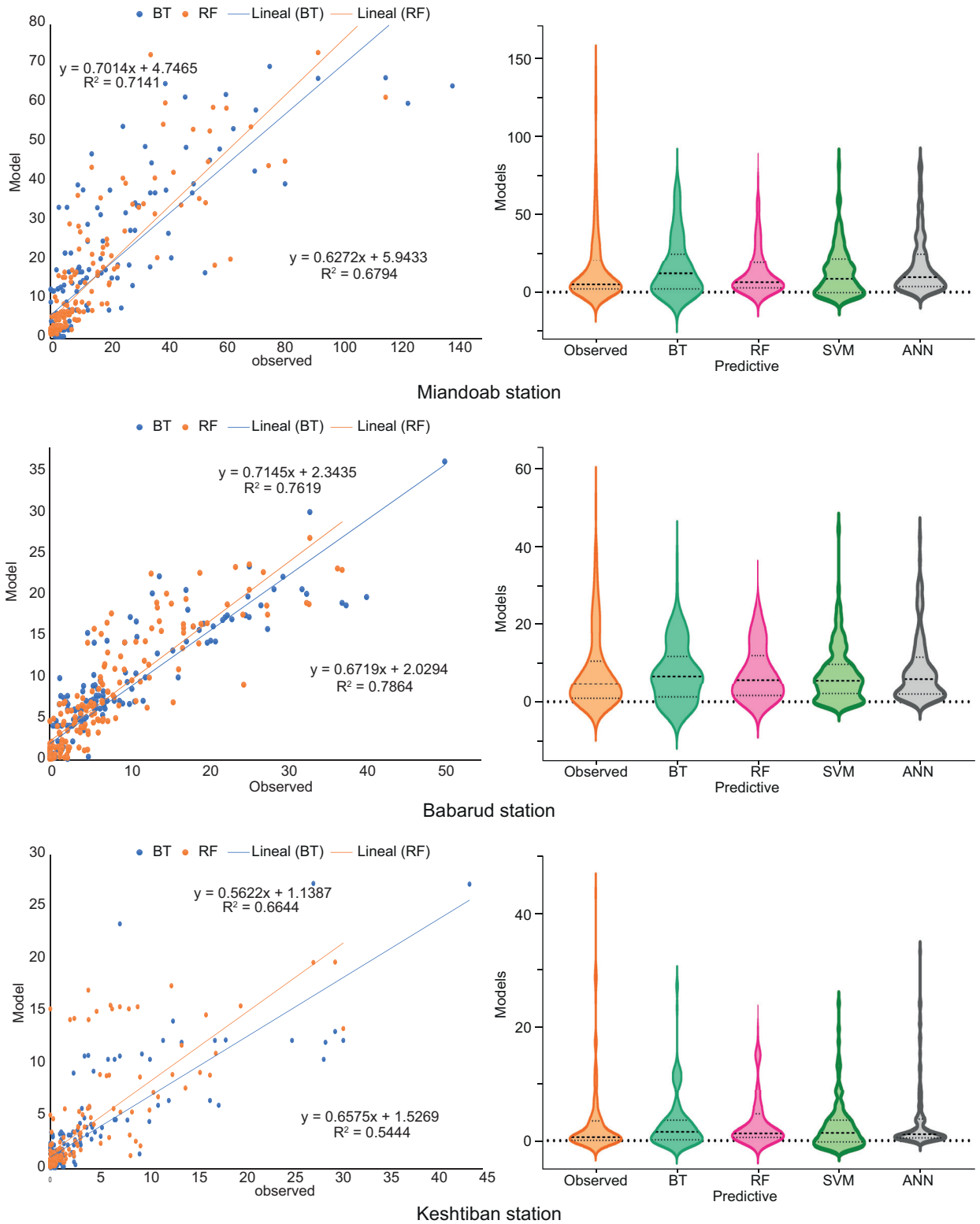

Fig. 8. Verification scatter plots and violin plots of simulated runoff using the Random Forest (RF) and Boosted Tree (BT) models in the western sub-basin.

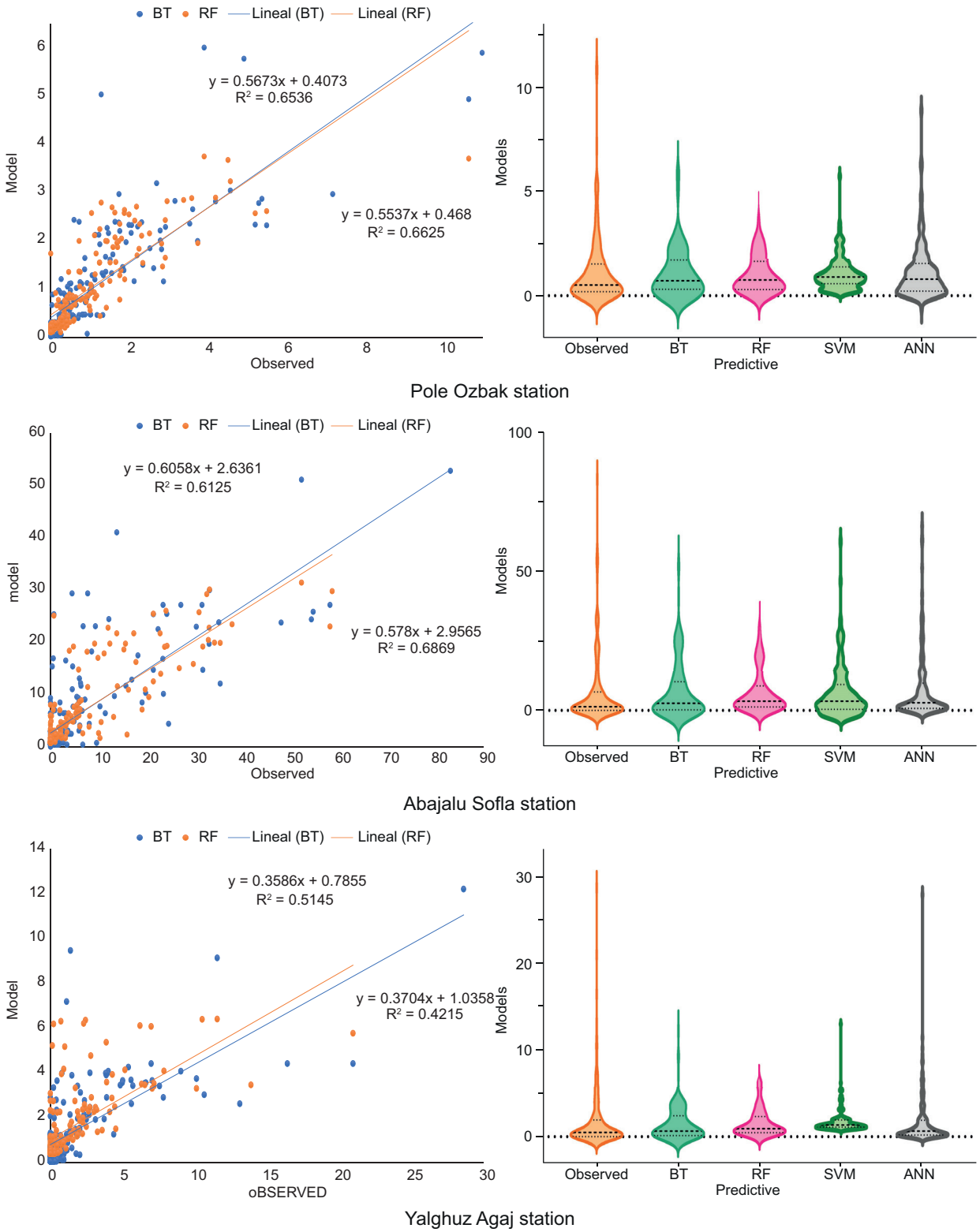

Fig. 8. Verification scatter plots and violin plots of simulated runoff using the Random Forest (RF) and Boosted Tree (BT) models in the western sub-basin.

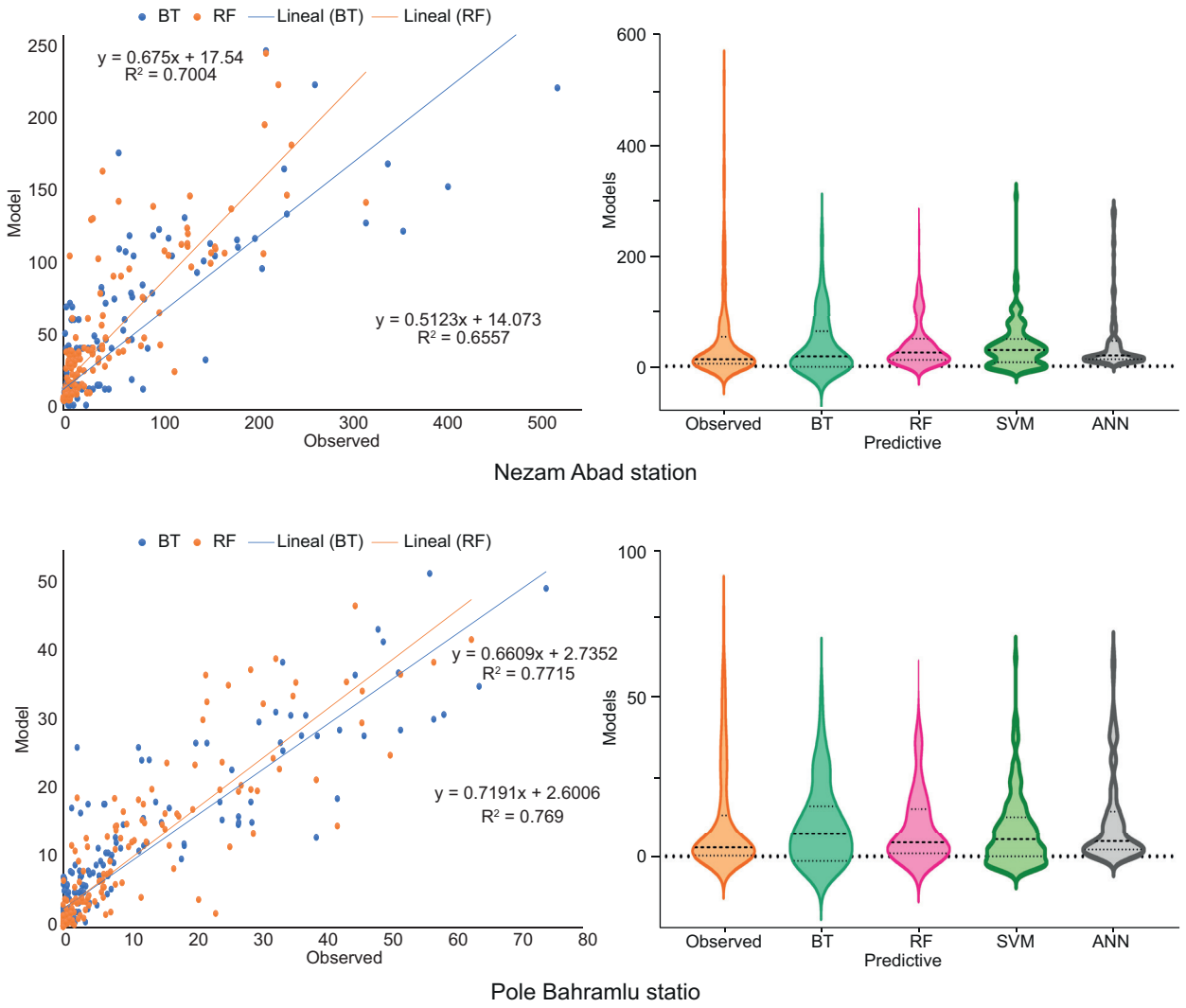

Fig. 8. Verification scatter plots and violin plots of simulated runoff using the Random Forest (RF) and Boosted Tree (BT) models in the western sub-basin.

recent years. This reduction in runoff and inflow can be attributed to several factors, including increased urban water demand and extensive agricultural development, with the agricultural sector being the predominant consumer of water resources from the basin.

Acknowledgments

The authors express their gratitude to the Iran Meteorological Organization and the Regional Water Company of East Azerbaijan in Iran for granting access to the weather, hydrological, and agriculture databases of the study area.

References

Adnan RM, Liang Z, Heddam S, Zounemat-Kermani M, Kisi O, Li B. 2020. Least square support vector machine and multivariate adaptive regression splines for streamflow prediction in mountainous basin using hydro-meteorological data as inputs. Journal of Hydrology 586: 124371. https://doi.org/10.1016/j.jhydrol.2019.124371

Ahmadaali J, Barani GA, Qaderi K, Hessari B. 2018. Analysis of the effects of water management strategies and climate change on the environmental and agricultural sustainability of Urmia Lake basin, Iran. Water 10: 160. https://doi.org/10.3390/w10020160

Aktürk G, Yıldız O. 2018. Çatalan Baraj Havzasında Yağış Eksikliğinin Çeşitli Hidrolojik Sistemler Üzerine Etkileri (The effect of precipitation deficits on hydrological systems in the Çatalan Dam basin, Turkey). International Journal of Engineering Research and Development 10: 10-28. https://doi.org/10.29137/umagd.441389

Ali S, Shahbaz M. 2020. Streamflow forecasting by modeling the rainfall-streamflow relationship using artificial neural networks. Modeling Earth Systems and Environment 6: 1645-1656. https://doi.org/10.1007/s40808-020-00780-3

Alizade Govarchin Ghale Y, Baykara M, Unal A. 2019. Investigating the interaction between agricultural lands and Urmia Lake ecosystem using remote sensing techniques and hydro-climatic data analysis. Agricultural Water Management 221: 566-579. https://doi.org/10.1016/j.agwat.2019.05.028

Alizadeh MJ, Kavianpour MR, Kisi O, Nourani V. 2017. A new approach for simulating and forecasting the rainfall-runoff process within the next two months. Journal of Hydrology 548: 588-597. https://doi.org/10.1016/j.jhydrol.2017.03.032

Asadi H, Shahedi K, Jarihani B, Sidle RC. 2019. Rainfall-runoff modelling using hydrological connectivity index and artificial neural network approach. Water 11: 212. https://doi.org/10.3390/w11020212

Aurenhammer F, Klein R, Lee DT. 2013. Voronoi diagrams and Delaunay triangulations. World Scientific Publishing Company, 346 pp. https://doi.org/10.1142/9789814447645_0001

Bashirian F, Rahimi D, Movahedi S, Zakerinejad R. 2020. Water level instability analysis of Urmia Lake basin in the northwest of Iran. Arabian Journal of Geosciences 13: 193. https://doi.org/10.1007/s12517-020-5207-1

Bigdeli Z, Majnooni-Heris A, Delirhasannia R, Karimi S. 2023. Application of Support Vector Machine and Boosted Tree algorithm for rainfall-runoff modeling (case study: Tabriz plain). Environment and Water Engineering 9: 532-547. https://doi.org/10.22034/ewe.2023.366913.1816

Bigdeli Z, Majnooni-Heris A, Delirhasannia R, Karimi S. 2024. Rain-runoff modeling of Khormazard and Bonab hydrometric stations using Support Vector Machine and Random Forest algorithms. Water and Soil 37: 971-989. https://doi.org/10.22067/jsw.2023.81608.1264

Breiman L. 2001. Random forests. Machine Learning 45: 5-32. https://doi.org/10.1023/A:1010933404324

Calver A. 1988. Calibration, sensitivity and validation of a physically-based rainfall-runoff model. Journal of Hydrology 103: 103-115. https://doi.org/10.1016/0022-1694(88)90008-X

Dawson CW, See LM, Abrahart RJ, Heppenstall AJ. 2006. Symbiotic adaptive neuro-evolution applied to rainfall-runoff modelling in northern England. Neural Networks 19: 236-247. https://doi.org/10.1016/j.neunet.2006.01.009

Farajzadeh J, Fakheri Fard A, Lotfi S. 2014. Modeling of monthly rainfall and runoff of Urmia Lake basin using "feed-forward neural network" and "time series analysis" model. Water Resources and Industry 7-8: 38-48. https://doi.org/10.1016/j.wri.2014.10.003

Friedman N, Goldszmidt M, Wyner A. 2013. Data analysis with Bayesian networks: A bootstrap approach. In: Proceedings of the Fifteenth Conference on Uncertainty in Artificial Intelligence (UAI1999). arXiv preprint arXiv 1301.6695. https://doi.org/10.48550/arXiv.1301.6695

Hamidi O, Poorolajal J, Sadeghifar M, Abbasi H, Maryanaji Z, Faridi HR, Tapak L. 2015. A comparative study of support vector machines and artificial neural networks for predicting rainfall in Iran. Theoretical and Applied Climatology 119: 723-731. https://doi.org/10.1007/s00704-014-1141-z

Hamidi-Razi H, Mazaheri M, Carvajalino-Fernández M, Vali-Samani J. 2019. Investigating the restoration of Lake Urmia using a numerical modelling approach. Journal of Great Lakes Research 45: 87-97. https://doi.org/10.1016/j.jglr.2018.10.002

Hassanzadeh E, Zarghami M, Hassanzadeh Y. 2012. Determining the main factors in declining the Urmia Lake level by using system dynamics modeling. Water Resources Management 26: 129-145. https://doi.org/10.1007/s11269-011-9909-8

Hosseini-Moghari SM, Araghinejad S, Tourian MJ, Ebrahimi K, Döll P. 2020. Quantifying the impacts of human water use and climate variations on recent drying of Lake Urmia basin: The value of different sets of spaceborne and in situ data for calibrating a global hydrological model. Hydrology and Earth System Sciences 24: 1939-1956. https://doi.org/10.5194/hess-24-1939-2020

Javadzadeh H, Ataie-Ashtiani B, Hosseini SM, Simmons CT. 2020. Interaction of lake-groundwater levels using cross-correlation analysis: A case study of Lake Urmia Basin, Iran. Science of The Total Environment 729: 138822. https://doi.org/10.1016/j.scitotenv.2020.138822

Karimi S, Shiri J, Marti P. 2020. Supplanting missing climatic inputs in classical and random forest models for estimating reference evapotranspiration in humid coastal areas of Iran. Computers and Electronics in Agriculture 176: 105633. https://doi.org/10.1016/j.compag.2020.105633

Kan G, Li J, Zhang X, Ding L, He X, Liang K, Jiang X, Ren M, Li H, Wang F, Zhang Z, Hu Y. 2016. A new hybrid data-driven model for event-based rainfall-runoff simulation. Neural Computing and Applications 28: 2519-2534. https://doi.org/10.1007/s00521-016-2200-4

Kendall MG. 1975. Rank correlation methods. 4th ed. Charles Griffin, London.

Kisi O, Parmar KS. 2016. Application of least square support vector machine and multivariate adaptive regression spline models in long term prediction of river water pollution. Journal of Hydrology 534: 104-112. https://doi.org/10.1016/j.jhydrol.2015.12.014

Kumar S, Roshni T, Himayoun D. 2019. A comparison of emotional neural network (ENN) and artificial neural network (ANN) approach for rainfall-runoff modelling. Civil Engineering Journal 5: 2120-2130. https://doi.org/10.28991/cej-2019-03091398

Lan Y. 2014. Forecasting performance of support vector machine for the Poyang Lake's water level. Water Science and Technology 70:1488-1495. https://doi.org/10.2166/wst.2014.396

Lari A, Pishvaee MS, Khodabakhsh P. 2019. A system dynamics approach for basin policy design: Urmia Lake case study. Kybernetes 49: 1691-1720. https://doi.org/10.1108/K-04-2019-0226

Lee H, McIntyre N, Wheater H, Young A. 2005. Selection of conceptual models for regionalisation of the rainfall-runoff relationship. Journal of Hydrology 312: 125-147. https://doi.org/10.1016/j.jhydrol.2005.02.016

Lee S, Kim JC, Jung HS, Lee MJ, Lee S. 2017. Spatial prediction of flood susceptibility using random-forest and boosted-tree models in Seoul metropolitan city, Korea. Geomatics, Natural Hazards and Risk 8: 1185-1203. https://doi.org/10.1080/19475705.2017.1308971

Lettenmaier DP, Wood EF, Wallis JR. 1994. Hydro-climatological trends in the continental United States, 1948 -88. Journal of Climate 7: 586-607. https://doi.org/10.1175/1520-0442(1994)007<0586:HCTITC>2.0.CO;2

Li M, Zhang Y, Wallace J, Campbell E. 2020. Estimating annual runoff in response to forest change: A statistical method based on random forest. Journal of Hydrology 589:125168. https://doi.org/10.1016/j.jhydrol.2020.125168

Mann HB. 1945. Non-parametric test against trend. Econometrica 13: 245-259. https://doi.org/10.2307/1907187

Meng C, Zhou J, Tayyab M, Zhu S, Zhang H. 2016. Integrating artificial neural networks into the VIC model for rainfall-runoff modeling. Water 8: 407. https://doi.org/10.3390/w8090407

Naghibi SA, Pourghasemi HR, Dixon B. 2016. GIS-based groundwater potential mapping using boosted regression tree, classification and regression tree, and random forest machine learning models in Iran. Environmental Monitoring and Assessment 188: 44. https://doi.org/10.1007/s10661-015-5049-6

Nazeri-Tahroudi M, Ahmadi F, Khalili K. 2018. Impact of 30 years changing of river flow on Urmia Lake basin. AUT Journal of Civil Engineering 2: 115-122. https://doi.org/10.22060/AJCE.2018.14520.5481

Nordberg H, Cantor M, Dusheyko S, Hua S, Poliakov A, Shabalov I, Smirnova T, Grigoriev IV, Dubchak I. 2014. The genome portal of the Department of Energy Joint Genome Institute: 2014 updates. Nucleic Acids Research 42: D26-D31. https://doi.org/10.1093/nar/gkt1069

Norouzi H, Nadiri AA, Asghari Moghaddam A, Norouzi M. 2018. Comparing performants of fuzzy logic, artificial neural network and random forest models in transmissivity estimation of Malekan plain aquifer. Iranian Journal of Ecohydrology 5: 739-751. https://doi.org/10.22059/IJE.2018.239914.707

Nylén T, Hellemaa P, Luoto M. 2014. Determinants of sediment properties and organic matter in beach and dune environments based on boosted regression trees. Earth Surface Processes and Landforms 40: 1137-1145. https://doi.org/10.1002/esp.3698

Obasi AA, Ogbu KN, Orakwe LC, Ahaneku IE. 2020. Rainfall-river discharge modelling for flood forecasting using Artificial Neural Network (ANN). Journal of Water and Land Development 44: 98-105. https://doi.org/10.24425/jwld.2019.127050

Park D, Markus M. 2014. Analysis of a changing hydrologic flood regime using the Variable Infiltration Capacity model. Journal of Hydrology 515: 267-280. https://doi.org/10.1016/j.jhydrol.2014.05.004

Pasquini AI, Lecomte KL, Piovano EL, Depetris PJ. 2006. Recent rainfall and runoff variability in central Argentina. Quaternary International 158: 127-139. https://doi.org/10.1016/j.quaint.2006.05.021

Petrasova A, Harmon B, Petras V, Tabrizian P, Mitasova H. 2015. Tangible modeling with open-source GIS. Springer International Publishing, New York, USA. https://doi.org/10.1007/978-3-319-25775-4

Sabouhi R, Soltani S. 2008. Analysis of the climate trend in the major cities of Iran. Journal of Agricultural Science and Technology 12: 46 (in Persian).

Salehi Bavil S, Zeinalzadeh K, Hessari B. 2018. The changes in the frequency of daily rainfall in Urmia Lake basin, Iran. Theoretical and Applied Climatology 133: 205-214. https://doi.org/10.1007/s00704-017-2177-7

Serrano A, Mateos VL, García JA. 1999. Trend analysis of monthly precipitation over the Iberian Peninsula for the period 1921-1995. Physics and Chemistry of the Earth, Part B: Hydrology, Oceans and Atmosphere 24: 85-90. https://doi.org/10.1016/S1464-1909(98)00016-1

Shekar S, Xiong H. 2007. Encyclopedia of GIS. Springer Science & Business Media, New York, USA, LXXVIII, 1370 pp. https://doi.org/10.1007/978-0-387-35973-1

Shiri J. 2019. Prediction vs. estimation of dewpoint temperature: Assessing GEP, MARS and RF models. Hydrology Research 50: 633-643. https://doi.org/10.2166/nh.2018.104

Singh A, Malik A, Kumar A, Kisi O. 2018. Rainfall-runoff modeling in hilly watershed using heuristic approaches with gamma test. Arabian Journal of Geosciences 11: 261. https://doi.org/10.1007/s12517-018-3614-3

Sun Y, Niu J, Sivakumar B. 2019. A comparative study of models for short-term streamflow forecasting with emphasis on wavelet-based approach. Stochastic Environmental Research and Risk Assessment 33: 1875-1891. https://doi.org/10.1007/s00477-019-01734-7

Tan L, Scarton C, Specia L, van Genabith J. 2016. SAARSHEFF at SemEval-2016 task 1: semantic textual similarity with machine translation evaluation metrics and (eXtreme) boosted tree ensembles. In: Proceedings of the 10th International Workshop on Semantic Evaluation (SemEval-2016), 628-633. https://doi.org/10.18653/v1/S16-1095

Tariq Khan M, Shoaib M, Hammad M, Salahudin H, Ahmad F, Ahmad S. 2021. Application of machine learning techniques in rainfall-runoff modelling of the Soan River basin, Pakistan. Water 13: 3528. https://doi.org/10.3390/w13243528

Tayyab M, Zhou J, Dong X, Ahmad I, Sun N. 2019. Rainfall-runoff modeling at Jinsha River basin by integrated neural network with discrete wavelet transform. Meteorology and Atmospheric Physics 131: 115-125. https://doi.org/10.1007/s00703-017-0546-5

Turgay P, Ercan K. 2005. Trend analysis in Turkish precipitation data. Hydrological Processes: An International Journal 20: 2011-2026. https://doi.org/10.1002/hyp.5993

Turhan E, Keleş MK, Tantekin A, Keleş AE. 2019. The investigation of the applicability of data-driven techniques in hydrological modeling: The case of Seyhan basin. Rocznik Ochrona Środowiska 21: 29-51.

Turhan E. 2021. A Comparative evaluation of the use of artificial neural networks for modeling the rainfall-runoff relationship in water resources management. Journal of Ecological Engineering 22: 166-178. https://doi.org/10.12911/22998993/135775

Vaheddoost B, Aksoy H. 2018. Interaction of groundwater with Lake Urmia in Iran. Hydrological Processes 32: 3283-3295. https://doi.org/10.1002/hyp.13263

Vidyarthi VK, Jain A, Chourasiya S. 2020. Modeling rainfall-runoff process using artificial neural network with emphasis on parameter sensitivity. Modeling Earth Systems and Environment 6: 2177-2188. https://doi.org/10.1007/s40808-020-00833-7

Wang WC, Xu DM, Chau KW, Chen S. 2013. Improved annual rainfall-runoff forecasting using PSO-SVM model based on EEMD. Journal of Hydroinformatics 15: 1377-1390. https://doi.org/10.2166/hydro.2013.134